Supporting Information for:

Antibody conjugate assembly on ultrasound-confined microcarrier particles

Michael M. Binkley,[†] Mingyang Cui,[†] Mikhail Y. Berezin,[‡,§] and J. Mark Meacham[†,§,*]

[†]*Department of Mechanical Engineering and Materials Science at Washington University in St. Louis, MO*

[‡]*Department of Radiology at Washington University School of Medicine in St. Louis, MO*

[§]*Institute of Materials Science and Engineering at Washington University in St. Louis, MO*

[*]*Address: Washington University in St. Louis, 1 Brookings Drive, Jubel Hall, Room 203K, St. Louis, MO 63130; Phone: 314-935-3821; Email: meachamjm@wustl.edu*

Page count: 5
Figure count: 5

Microscale object manipulation and confinement in an ultrasonic standing wave field

Under an arbitrary applied acoustic field, the forces acting on a particle have been thoroughly detailed.[1-3] In an inviscid fluid, the primary radiation force ($\boldsymbol{F}_{ac}$) acting on a spherical particle of radius a can be expressed as a function of the first order pressure and velocity fields:

$$\boldsymbol{F}_{ac} = -\frac{4\pi}{3}a^3\nabla\left[f_1\frac{1}{2}\kappa_o\langle p_{in}^2\rangle - f_2\frac{3}{4}\rho_o\langle v_{in}^2\rangle\right], \quad (1)$$

where p_{in} and v_{in} are the incoming acoustic pressure and velocity fields at the particle location, $\langle\ \rangle$ denotes a time average over a full oscillation period of a time-harmonic quantity, and the compressibility (f_1) and density (f_2) coefficients account for the material property mismatch between the particle (subscript p) and the suspending medium (subscript o). These unitless coefficients are given by the following equations:

$$f_1 = 1 - \frac{\kappa_p}{\kappa_o} \text{ and} \quad (2)$$

$$f_2 = \frac{2(\rho_p - \rho_o)}{2\rho_p + \rho_o}, \quad (3)$$

where κ is the compressibility and ρ is the density. These two parameters can be summarized in the acoustic contrast factor Φ, defined by the following equation:

$$\Phi = \frac{f_1}{3} + \frac{f_2}{2}. \quad (4)$$

Thus, the acoustic contrast factor can take on a positive, negative, or zero value depending on the material properties of the particle and medium. The direction of the force is given by the sign of the acoustic contrast factor with particles exhibiting positive (negative) Φ moving towards regions of low (high) pressure. A zero Φ will result in no acoustic radiation force in the direction of a node or antinode.

Experimental setup for in-channel synthesis

Figure S1 shows the experimental setup used for microparticle substrate retention, and capture, modification, purification, and release of antibody (Ab) within the longitudinal standing bulk acoustic wave (LSBAW) microreactor. The 63.5 mm × 63.5 mm × 1.5-mm thick glass LSBAW chip included two microchannels positioned adjacent to one another. A 24 mm × 28 mm × 1.5-mm thick piezoelectric transducer (PZT element in **Figure S1a**; APC 880, American Piezo Ceramics, Inc.) was mechanically clamped over the unused microchannel with a thin layer of ultrasound gel (McKesson Corp.) applied as an acoustic coupling layer to facilitate wave propagation. Fluids were introduced into the LSBAW microchannel via syringe pump (Legato 110, KD Scientific, Inc.) under the prescribed flowrate (7 µL/min). Tubing was tightly held against the 1-mm diameter drilled inlet/outlet ports using microfluidic probes (CorSolutions, LLC). An amplified ac signal (33522A, Agilent Technologies, Inc.; 2100L, Electronic Navigation Industries) was used to drive the PZT element at the experimentally determined first half-wavelength resonance of the microreactor shown in **Figure S1b**. The assembled experimental setup was held in a custom laser cut acrylic holder over an inverted microscope (**Figure S1a**; Axio Observer z.1, Carl Zeiss AG) for both brightfield and fluorescence imaging.

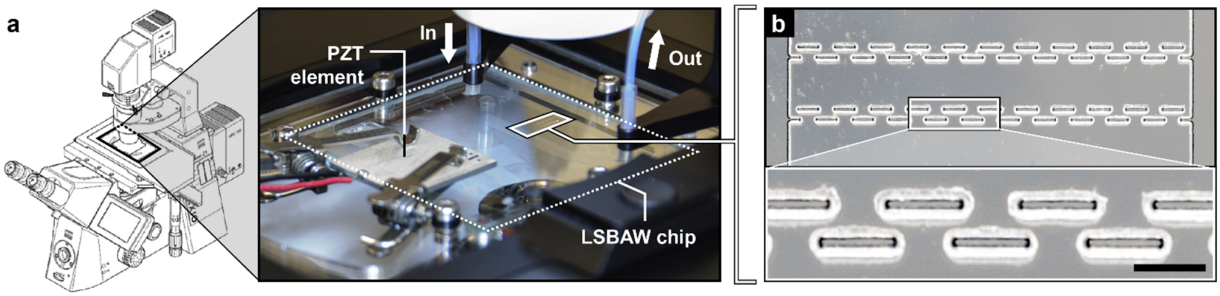

Figure S1. Experimental setup for synthesis of antibody conjugates within the LSBAW microreactor. (**a**) Oblique view of the LSBAW chip actuated by a piezoelectric transducer and mounted on the stage of an inverted microscope. (**b**) Isotropically etched glass pillar arrays for the augmentation and enhancement of the local pressure field within the microreactor. Scale bar is 500 µm.

Hollow glass sphere surface chemistry development and verification

Demonstration of antibody (Ab) binding to the microparticle substrate was conducted manually outside of the LSBAW channel. Functionalization of hollow glass spheres (HGSs, 6 µm ± 3.5 µm diameter; HGS-10, Dantec Dynamics A/S) was based on a previously reported protocol for treatment of silicon surfaces to immobilize proteins.[4] The HGS functionalization and labeling procedure is outlined in **Figure S2**. Briefly, (**a**) HGSs were incubated in a mixture of conc. H_2SO_4 (98%) and H_2O_2 (aq., 30%) 3:1 (vol.) for 2 h to produce open surface hydroxyl groups, (**b**) hydroxyl groups were silanized using 1% (v/v) 3-aminopropyltriethoxysilane (APTES, Sigma-Aldrich, Inc.) in anhydrous ethanol for 10 min under constant agitation, (**c**) APTES was activated with 5% (v/v) glutaraldehyde (Sigma-Aldrich) in phosphate buffered saline solution (1xPBS, Thermo Fisher Scientific, Inc.) for 3 h after APTES evaporation at 100°C for 1 h, and (**d**) Protein G was coupled to the activated surface by incubating HGS in a solution of recombinant Protein G from *G. Streptococci* (1 mg/mL in PBS; Sigma Aldrich) at 4°C for 3 h. Verification of reaction chemistry was shown by incubating Protein G-terminated HGS with fluorescent antibody (5 µg/mL in 1xPBS; rabbit anti-goat IgG Alexa Fluor 488, Abcam, Inc.) for 1 h at 4°C. **Figures S2f** and **S2g** are a brightfield image of the untreated HGSs and a fluorescence image of the activated HGSs with coupled Abs (aHGS), respectively.

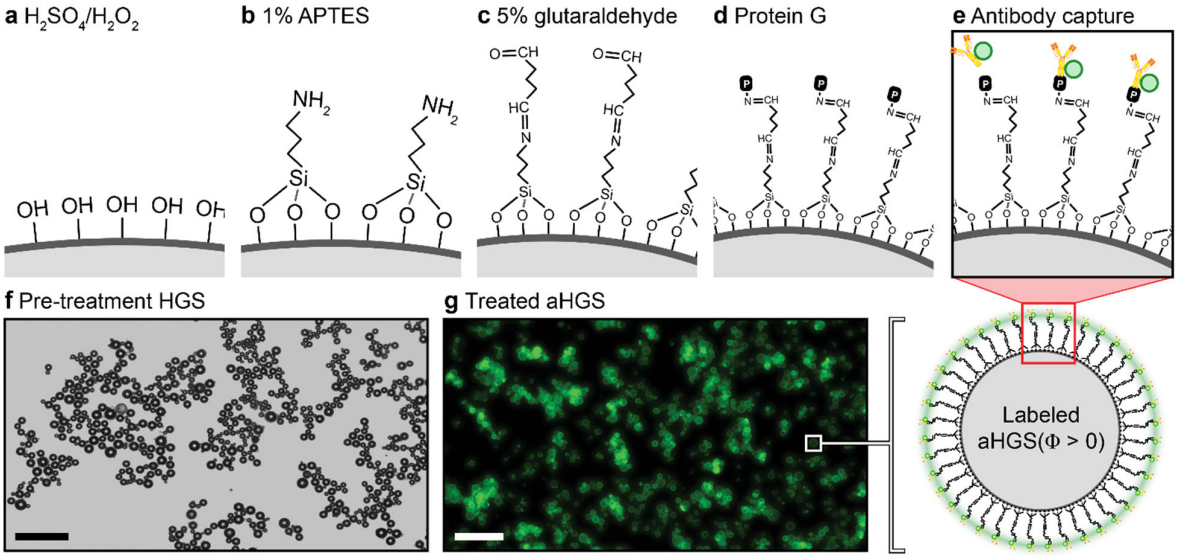

Figure S2. Hollow glass sphere (HGS) functionalization and antibody-labeling protocol. (**a**) Formation of hydroxyl groups on the surface by suspension of beads in a solution of conc. H_2SO_4 (98%) and H_2O_2 (aq., 30%) 3:1 (vol.). (**b**) Production of open surface amines via addition of 1% (v/v) APTES in anhydrous ethanol. (**c**) APTES activation using 5% (v/v) glutaraldehyde in 1xPBS. (**d**) Coupling of Protein G (1 mg/mL in 1xPBS) to activated surface. (**e**) Efficacy of reaction was demonstrated using fluorescently tagged antibodies (5 µg/mL) diluted in 1xPBS. (**f**) Brightfield image of pre-treatment HGSs and (**g**) fluorescence image of treated aHGS (t_{exp} = 3 sec). Scale bars are 50 µm.

Assessment of antibody degradation following ultrasound exposure

To determine whether ultrasound exposure in the LSBAW microreactor effects a change in the molecular weight of the antibodies (Abs), samples treated under three different conditions were analyzed using gel electrophoresis. Samples were aliquoted directly from a stock solution of fluorescent Ab (2 mg/mL in 1xPBS; rabbit anti-goat IgG Alexa Fluor 488, Abcam) and stored at 4°C. The primary control C_1, was left untreated at 4°C for the duration of the experiment. The second control C_2, was taken from the stock solution and introduced into the LSBAW microchannel at a flow rate of 7 µL/min for ~15 min yielding a final sample volume of 50 µL. C_2 served as a flow control to determine whether exposure to fluid shear within the device might adversely affect the Ab structure. Finally, sample E_1 represented the experimental analog, which was introduced into the channel at a flow rate of 7 uL/min for 7 min during actuation at the experimental drive frequency and amplitude ($f_{1,E}$ = 575 kHz, V_E = 91 V_{pp}). The Ab-loaded LSBAW microreactor was left to sit at room temperature for 45 min prior to an additional 7 min of acoustic actuation representing the conditions experienced during PBS wash. Finally, sample E_1 was withdrawn at a flow rate of 7 µL/min until a final solution volume of 40 µL was collected.

Three dilutions of each sample were prepared (1 mg/mL, 0.67 mg/mL, and 0.40 mg/mL, with deionized water). 12 µL of each of the nine samples was loaded into the precast Invitrogen Novex 4-20% Tris-Glycine Mini Gel (Thermo Fisher Scientific) with 4 µL of 4x NuPAGE LDS Sample Buffer (Thermo Fisher Scientific). For estimation of the molecular

weight, 10 µL of Spectra Multicolor Broad Range Protein Ladder (Thermo Fisher Scientific) was placed in the first well. The gel was then immersed in a 19:1 mixture of deionized water and 20x NuPAGE MES SDS Running Buffer (Thermo Fisher Scientific) and run for 25 min at 200 V (PowerPac Basic Power Supply, Bio-Rad Laboratories, Inc.). The gel was then washed with deionized water and patted dry before results were recorded using an in-house imager. **Figure S3** indicates that bands are consistent across all nine samples with a molecular weight greater than 130 kDa.

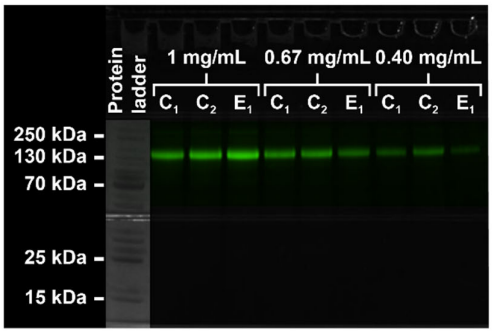

Figure S3. Composite picture of brightfield and fluorescence images of gel electrophoresis results. Protein molecular weights of interest are labeled on the protein ladder. From left to right: protein ladder, 1 mg/mL C_1 sample, 1 mg/mL C_2 sample, and 1 mg/mL E_1 sample; 0.67 mg/mL C_1 sample, 0.67 mg/mL C_2 sample, and 0.67 mg/mL E_1 sample; and 0.40 mg/mL C_1 sample, 0.40 mg/mL C_2 sample, and 0.40 mg/mL E_1 sample. Fluorescence image taken at 6 sec exposure.

Comparative imaging of pretreatment and modified samples

Analysis of flow cytometry showed partial fluorescence of Protein G-coated HGSs in both the green and red channels. Fluorescence images of a focused Protein G-terminated HGS sample confined within the LSBAW microreactor were taken using the same parameters as for a modified (double-labeled) bead cluster to determine if fluorescence was an artifact of exposure time or was due to Ab coupling and Cy3 labeling. **Figure S4** shows the brightfield, green/FITC channel, and red/Cy3 channel images of the pretreatment control and modified clusters. Note that the synthesis progression resulting in the cluster of **Figure S4d-f** was identical to that yielding the cluster shown in the inset of **Figure 5b**. Lack of Protein G fluorescence under the given exposure conditions indicates that fluorescence found in the modified sample is a result of Alexa Fluor 488 (AF488) and Cy3 labeling rather than Protein G fluorescence.

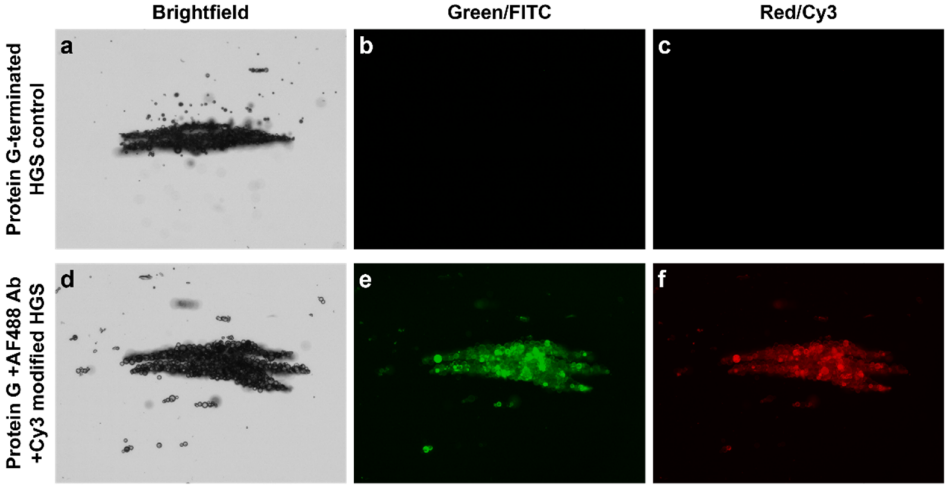

Figure S4. Brightfield and fluorescence images of an unmodified Protein G-terminated bead cluster and a LSBAW microreactor-modified HGS cluster. The unmodified Protein G-terminated control is focused between pillar arrays of the microreactor and imaged in (**a**) brightfield (t_{exp} = 0.25 sec), (**b**) green/FITC channel (t_{exp} = 2 sec), and (**c**) red/Cy3 channel (t_{exp} = 2 sec). The modified cluster is focused between pillar arrays of the microreactor and imaged in (**d**) brightfield (t_{exp} = 0.25 sec), (**e**) green/FITC channel (t_{exp} = 2 sec), and (**f**) red/Cy3 channel (t_{exp} = 2 sec).

Flow cytometry control samples

Quantification of fluorescent antibody and fluorophore binding was conducted using flow cytometry (LSR Fortessa, BD Biosciences) and the analysis software FlowJo v.10 (FlowJo, LLC). Five control samples and one LSBAW microreactor-

assembled sample were prepared to assess reagent effects on bead stability and fluorescence. A solution of bare HGSs was diluted in 1xPBS ($4x10^7$ beads/mL) to serve as an unmodified control (Con1). Protein G-terminated HGSs were prepared as described above (**Figure S2a-d**) and suspended in 1xPBS to a final concentration of $4x10^7$ beads/mL to serve as a second bead control (Con2). Two additional bead controls (Con3 and Con4) were prepared for use as reference solutions for antibody-terminated HGSs (Con3, **Figure S2a-e**; green/FITC channel intensity) and to determine the extent to which the fluorescent Cy3 dye bound the Protein G-terminated HGS (Con4; red/Cy3 channel intensity). Con4 was prepared by incubating Protein G-terminated HGSs in a solution of sulfo-Cyanine3 (Cy3)-NHS ester (2 mg dye per 1 mL of pH 8.0 buffer) for 4 h prior to wash and resuspension in 1xPBS to a final concentration of $4x10^7$ beads/mL. The final control (Con5) was a Cy3 treated fluorescent antibody-terminated HGS created using manual synthesis with a 4 h Cy3 incubation added after the steps outlined in **Figure S2a-e**, and resuspension to $4x10^7$ beads/mL in 1xPBS. The LSBAW microreactor-assembled sample was pooled from three collections of double-labeled beads created using the LSBAW-based synthesis detailed in the main text of the manuscript. This solution was centrifuged and resuspended to a final concentration of $9x10^4$ beads/mL.

The Con5 solution was used to calibrate the intensity of the flow cytometer to ensure all beads remained in the collection range with no saturation. The maximum signal allowed for Con5 was set to $1x10^4$ for both the blue and yellow/green excitation channels (corresponding to green and red emission). Four channels of data were collected: (1) Forward Scatter (FSC-A), $V_{excitation}$ = 654 V, (2) Side Scatter (SSC-A), $V_{excitation}$ = 258 V, (3) blue laser (FITC), λ_{ex} = 488 nm, dichroic filter: 505 nm LP, bandpass filter: 530/30 nm, $V_{excitation}$ = 351 V, and (4) yellow/green laser (Cy3), λ_{ex} = 552 nm, dichroic filter: 585 nm LP, bandpass filter: 585/15 nm, $V_{excitation}$ = 419 V. A total count of 10,000 particles was collected for all samples with no gating applied to the final sample populations. Flow cytometry intensity scatter plots for all cases are shown in **Figure S5**.

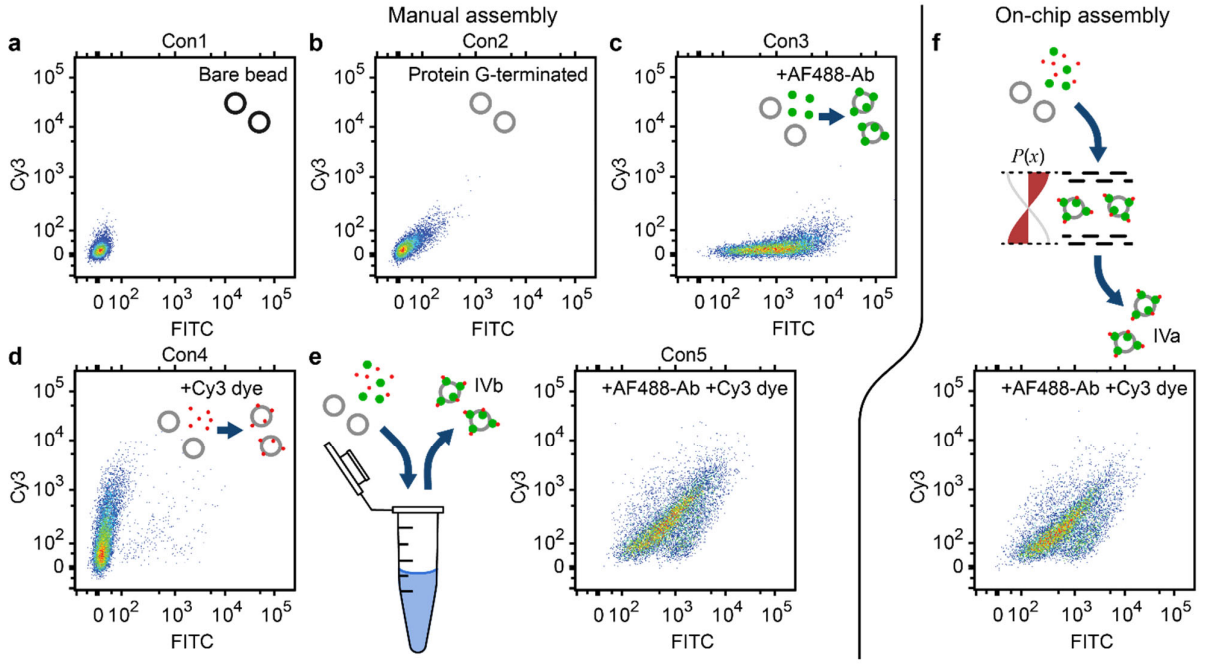

Figure S5. Flow cytometry results comparing relative Cy3 intensity (yellow/green excitation channel) to FITC intensity (blue excitation channel) for Con1-5 and an LSBAW microreactor-assembled sample. In order: (**a**) bare bead solution (Con1), (**b**) Protein G-terminated bead solution (Con2), (**c**) antibody-terminated bead solution (Con3), (**d**) Cy3 modified, Protein G-terminated bead solution (Con4), (**e**) manually Cy3 modified, antibody-terminated bead solution (Con5), and (**f**) LSBAW microreactor-Cy3 modified, antibody-terminated bead solution.

References

1. L. Gor'kov, Doklady Akademii Nauk SSSR **1961,** 140, 88.
2. K. Yosioka and Y. Kawasima, Acta Acustica united with Acustica **1955,** 5, 167-173.
3. H. Bruus, Lab on a Chip **2012,** 12, 1014-1021.
4. L. M. Lee, R. L. Heimark, J. C. Baygents and Y. Zohar, Nanotechnology **2006,** 17, S29.